

Antoine FOURMAUX
Office National d'Etudes et de Recherches Aéropatiales
BP 72 - 92322 Châtillon Cedex, France

Abstract

This paper describes a two-dimensional unsteady calculation method which applies to the flow computation in two blade-rows, one being fixed, the other moving. The Euler equations are solved using the classical predictor-corrector McCormack scheme. The program can be used in many cases involving time-dependent phenomena : mutual influence of two blade-rows, distortion problems, wake passage effects, aeroelasticity. First, the computational program is described with a special importance being given to the boundary-conditions. Then, calculation examples are shown which allow one to evaluate the potential of this method for a detailed unsteady flow analysis.

I. Introduction

Generally speaking, in a turbomachine stage, the fluid is viscous and the flow is three-dimensional and unsteady. Thus such a flow is governed by the Navier-Stokes equations.

The numerical prediction of such a flow greatly depends on the available computers. The increasing power and rapidity of computer makes it possible to run more and more complicated calculations and hence to help research in ways which until recently were unthinkable.

One of these ways is the detailed study of time-dependent phenomena. For the previous mentioned reasons, few studies on this topic have been carried out, especially for supersonic and transonic flows. In their report, Erdos and Alzner⁽¹⁾ describe a two-dimensional method for the flow computation in a compressor stage. The use of phase-lagged boundary-conditions makes it possible to compute the flow over only one blade-to-blade passage of each wheel. More recently, Hodson⁽²⁾ computed a wake-generated unsteady flow in a turbine cascade.

In this paper, a two-dimensional unsteady calculation method will be presented. It can be used in several blade-to-blade passages of a unique blade-row or in two blade-rows having different angular speeds. Compressible inviscid fluid flows are computed by solving the Euler equations.

Several kinds of unsteady effects, such as mutual influence of two blade-rows, circumferential inlet distortion, aeroelasticity can be taken into account by suitable boundary-conditions.

II. Description of the computation method

II.1. Outline

The computation method is actually derived from time-marching codes solving the Euler equations⁽³⁾, ⁽⁴⁾.

Copyright © 1986 by ICAS and AIAA. All rights reserved.

In order to take into account variations of the stream surface radius and the channel height (AVDR effect), the Euler equations are written in the following way⁽³⁾ :

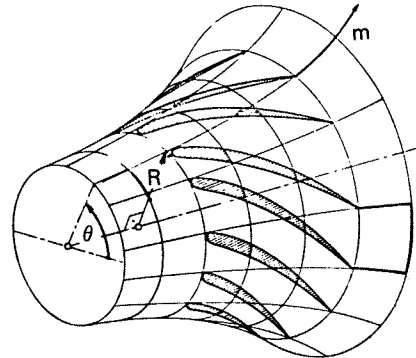


Figure 1. Flow coordinates.

m : meridional curvilinear abscissa (fig. 1)
theta : circumferential coordinate

- mass

$$\frac{\partial (br\rho)}{\partial t} + \frac{\partial (br\rho u)}{\partial m} + \frac{\partial (b\rho v)}{\partial \theta} = 0$$

- momentum

$$\frac{\partial (br\rho u)}{\partial t} + \frac{\partial (br(p + \rho u^2))}{\partial m} + \frac{\partial (b\rho uv)}{\partial \theta} =$$

$$p \frac{d(br)}{dm} + b\rho(v + \omega r)^2 \frac{dr}{dm}$$

$$\frac{\partial (br\rho v)}{\partial t} + \frac{\partial (br\rho uv)}{\partial m} + \frac{\partial (b(p + \rho v^2))}{\partial \theta} =$$

$$- b\rho u(v + 2\omega r) \frac{dr}{dm}$$

- energy

$$\frac{\partial (br(\rho J - p))}{\partial t} + \frac{\partial (br\rho u J)}{\partial m} + \frac{\partial (b\rho v J)}{\partial \theta} = 0$$

where :

- u : meridional velocity
- v : tangential velocity
- b : channel height
- rho : density
- p : static pressure
- J : rothalpy
- r : radius, function of m
- omega : angular speed.

These equations are discretized directly in the physical plane (m, theta) and then are solved by the McCormack scheme⁽⁵⁾.

Development and analysis of this numerical method were initially achieved at ONERA by Viviani and Veuillot⁽⁴⁾.

II.2. Computation domain and boundary-conditions

The choice of the computation domain where the above equations will be solved, and the choice of the boundary conditions depend on the final solution to be obtained :

In the special case where the solution is a settled periodic one, a reduced computation domain may be used : it will represent only one blade-to-blade passage of each wheel(1). The periodic unsteady flow will be achieved by applying unsteady boundary conditions. Of course, these conditions will be settled periodic ones. A judicious use of phase-lag properties makes this technique possible, and CPU memory and time needs are very reasonable.

But, more generally, if transient flows have to be computed, the above technique is no longer applicable. In this case, the computation domain must include the whole wheel (or all of the wheels) -in the 3-D case, or all of the blade-to-blade passages -in the 2-D case. So, the boundaries of such a domain are only the following : blade-boundaries, upstream and downstream boundaries in the 2-D case with the addition of the hub and tip walls for the 3-D case.

CPU memory and time requirements are, of course, rather large, but such calculations can be run on the existing powerful computers.

In this paper, the second way is chosen, and the computation domain includes the N_1 blade-to-blade passages of the first wheel, and the N_2 of the second one.

A first necessary condition is that the circumferential extension of the domain be the same for both the blade-rows, i.e. :

$$N_1 \times \text{pitch}_1 = N_2 \times \text{pitch}_2$$

N_1 , pitch_1 : blade-to-blade passage number and pitch of the first row
 N_2 , pitch_2 : blade-to-blade passage number and pitch of the second row.

During the computation, all the blade-to-blade passages pass together the different numeric scheme steps at each iteration. However, they are considered as $n = N_1 + N_2$ separated domains and suitable boundary conditions are applied to every domain (fig. 2).

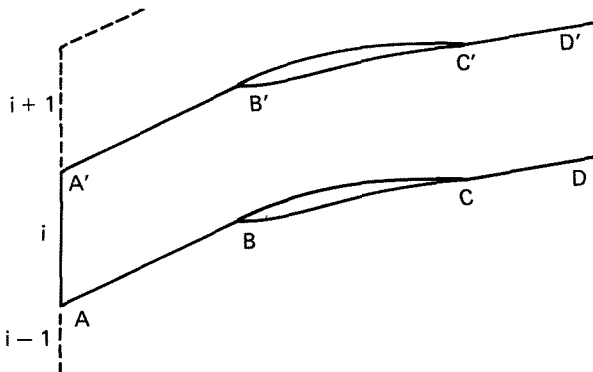


Figure 2. Boundary definition for a blade-to-blade passage.

For the most part, these conditions use compatibility relations (4) and (6) written in the local frame of reference where the unit normal vector is inward. For a two-dimensional flow, four relations are available.

$$p^{(n+1)} - (\rho a)^{(n)} V_n^{(n+1)} = p^* - (\rho a)^{(n)} V_n^* \quad (\text{C.R. 1})$$

$$p^{(n+1)} - (a^2)^{(n)} \rho^{(n+1)} = p^* - (a^2)^{(n)} \rho^* \quad (\text{C.R. 2})$$

$$V_t^{(n+1)} = V_t^* \quad (\text{C.R. 3})$$

$$p^{(n+1)} + (\rho a)^{(n)} V_n^{(n+1)} = p^* + (\rho a)^{(n)} V_n^* \quad (\text{C.R. 4})$$

where :

p : static pressure
 ρ : density
 a : sound velocity
 V : velocity component (in the local frame)

Subscripts :

n : normal to the boundary
 t : tangential to the boundary

Superscripts :

(n) , $(n+1)$: relative to the n th, $n + 1$ th iteration

$*$: value given by the numerical scheme.

According to the normal velocity sign and modulus, 1 relations may be used, and m conditions must be imposed, with $1 + m = 4(6)$.

II.2.1. Upstream boundary (AA')

The upstream boundary is parallel to the cascade front-line and the normal velocity is subsonic. Then only (C.R. 1) is used, if this boundary is the first blade-row one, and the following conditions are imposed :

- total pressure p_i
- total temperature T_i
- tangential velocity V_{t_i} .

These conditions may be uniform (uniform inlet flow) or non-uniform (distortion problem).

For the second row upstream boundary, the same technique can be used and inlet conditions are given by the first row outlet flow. However, another method -less expensive in computation time- is used and will be described in section II.2.6.

II.2.2. Upstream from the leading edge boundaries ($A_i B_i$, $A_i' B_i'$)

Through these boundaries, the flow is circumferentially continuous. Compatibility relations can be used, but in this simple case, they are replaced by transferring the results :

Conditions on $A_i' B_i'$ given by conditions on

$A_{i+1} B_{i+1}$ after predictor step.

Conditions on $A_i B_i$ given by conditions on

$A_{i-1} B_{i-1}$ after corrector step.

Of course, by using the spatial periodicity, fictitious $n+1$ th passage is the same as the first one ; this fact gives the upper boundary $A_n' B_n'$ and lower boundary $A_1 B_1$ conditions.

II.2.3. Blade boundaries (BC, B'C'). A slip condition is applied, i.e., the velocity normal to the blade must be zero. Hence, three relations (C.R. 1, C.R. 2, C.R. 3) are available.

II.2.4. Downstream form the trailing edge boundaries ($C_i D_i, C'_{i-1} D'_{i-1}$). At the beginning of the computation, these boundaries can be any boundaries whatsoever. At each iteration, they are moved and gradually become unsteady slip lines.

Through these lines, some discontinuities will appear, according to the Euler equations, and are expected to be correctly given by this technique.

In order to obtain the slip lines, a first possibility is the following: the slip condition (previously described) is applied to any point on the line $C_i D_i$, and to the same geometrical point of $C'_{i-1} D'_{i-1}$. However, both these points are not located exactly on the slip line, and in general, the static pressure has not the same value. So it would be necessary to move the $C_i D_i$ (and $C'_{i-1} D'_{i-1}$) boundary up to the slip line.

As a matter of fact, a more efficient treatment has been found: compatibility equations are used on $C_i D_i$ and $C'_{i-1} D'_{i-1}$ with two additional conditions, namely equality of the static pressure and equality of the velocity normal to the boundary. In this case, the normal velocity is not quite zero if the boundary is not the slip line and it allows us to define a "mesh displacement velocity" which is used throughout the computation to define a new mesh grid downstream from the trailing edges at each time step. Up to now, this treatment has been satisfactory because the normal velocity maintains a very low value from one iteration to another.

On the other hand, flow discontinuities through the slipstream continue down to the downstream boundary. This is not a problem when a single blade row is computed, but numerical difficulties may occur when the first row wake has to be introduced in the second row. As a matter of fact, upstream boundary conditions may be circumferentially non uniform, but they must be continuous. To avoid the problem caused by discontinuity, a mixing process, replacing pure discontinuities by strong local gradients, is applied to the very last mesh points of the slip line.

Because of its physical aspect, this treatment has very little influence on the blade-to-blade flow, and avoids numerical problems in the second row flow computation.

II.2.5. Downstream boundary (DD'). Downstream from the computation domain, the velocity normal to the boundary is subsonic, and in this case three compatibility equations are used, namely C.R. 1, C.R. 2 and C.R. 3.

A fourth condition is needed:

It can be provided by a static pressure condition, e.g., constant back pressure.

But it is also possible to use a fourth compatibility relation:

$$p^{(n+1)} + (\rho a)^{(n)} V_n^{(n+1)} = p^{(n)} + (\rho a)^{(a)} V_n^{(n)}$$

It is known as the "non reflecting boundary condition" and is interesting when the previous condition (constant back pressure) is considered unsuitable. However, the final solution is linked to the initial flow field, and sometimes some minor difficulties may occur in the final solution near the downstream boundary.

II.2.6. Linkage of both the domains. When the computation domain includes two wheels having different angular speeds, the flow in each wheel is computed within the relative frame of reference of the wheel.

Let D_1 be the upstream domain, and D_2 the downstream domain. In order to ensure flow continuity between D_1 and D_2 , the linkage of D_1 and D_2 has to be achieved on their common boundary.

This linkage is carried out within the computation and it does respect the numerical scheme.

Just after the predictor step, flow parameters computed on the upstream boundary of D_2 are translated from the D_2 frame of reference to the D_1 frame, and are applied to the downstream boundary of D_1 . During this process, the relative displacement of D_1 and D_2 is taken into account.

In a similar way, after the corrector step, the downstream conditions of D_1 are transmitted onto the upstream boundary of D_2 .

It is important to stress that this process is in perfect agreement with the McCormack scheme, since basically, the same technique is used on a common mesh line of D_1 or D_2 .

III. Periodic unsteady flows Period and frequency

In this paper, the method is applied to the flow calculation in a compressor stage and in a turbine stage, with uniform inlet and outlet conditions, in order to evaluate the effects of the vicinity of both wheels.

Hence, the unsteady flow is created only by the rotation (passage from one frame of reference to another), and it is a settle periodic flow. As the unsteady phenomenon frequencies are connected only to the angular speeds and to the blade numbers of wheels, we will say that these unsteadiness causes are "internal" ones.

As a matter of fact, if other "external" causes exist (such as periodic rotating stall), the frequencies of these phenomena will be superposed onto the internal frequencies of the machine. From a point of view other than the aerodynamic one, aeroelasticity problems can be classified as this second type.

Both of the following examples are cases of "internal" unsteady effects, although the same program may be used to compute cases of "external" effects⁽⁷⁾, or "internal" effects with an inlet distortion⁽⁸⁾.

The aerodynamic frequency of the flow parameters will now be emphasized in an example of a compressor stage (rotor + stator).

The rotor has N_r blades, and its angular speed is ω . The stator has N_s blades.

For the rotor in the relative frame of reference the period and the frequency are given by the stator. Their respective values are

$$f_r = \frac{|\omega| \times N_s}{2\pi} \quad T_r = \frac{1}{f_r} = \frac{2\pi}{|\omega| \times N_s}$$

Symmetrically, for the stator, in the absolute frame :

$$f_s = \frac{|\omega| \times N_r}{2\pi} \quad T_s = \frac{1}{f_s} + \frac{2\pi}{|\omega| \times N_r}$$

Numerically, $N_r = 48$, $N_s = 60$.

These blade numbers are not very realistic, because manufacturers generally choose N_r and N_s such as $HCF(N_r, N_s) = 1$ (H.C.F. : Highest Common Factor). However, many important criteria influence the choice of N_r and N_s , e.g., criteria involving aeroelastic features. Only from an aerodynamic point of view, it is expected that the flow fields will not be very different in these two stages :

The first one with $N_1 = 49$ $N_s = 59$
 (HCF (N_r, N_s) = 1)
 The second one with $N_1 = 48$ $N_s = 60$
 (HCF (N_1, N_s) = 12)

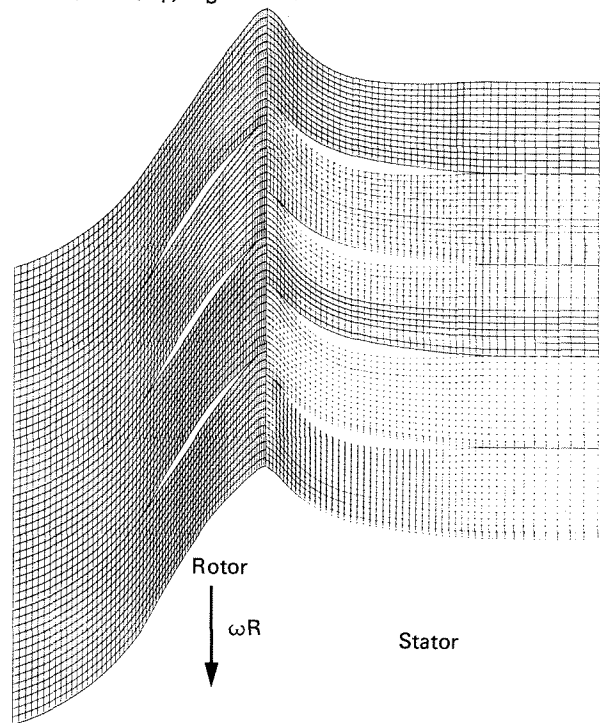


Figure 3. Compressor mesh grid.

In the second stage, a very high revolution symmetry exists which thus drastically reduces CPU memory and time and allows the computing of the flow in a domain including only 4 blade-to-blade passages for the rotor and 5 for the stator (fig. 3). A upper and lower boundary condition, the well known "spatial periodicity" condition is used (currently being taken advantage of in steady computations).

In a similar way, for the turbine stage, the following blade-numbers are chosen :

Stator : $N_s = 30$
 Rotor : $N_r = 50$ $HCF(N_s, N_r) = 10$

IV. Presentation and analysis of the results

IV.1. Compressor stage

The cascades are relative to the tip section of a single stage axial transonic compressor. For these sections, the machine radius is constant and the AVDR is equal to 1.

Upstream from the moving blade-row, the relative inlet Mach number is about 1.22 and the flow direction (relative to the axis) is about 60°.

An overall view of both the cascades is depicted on the mesh grid (fig. 3). For the first blade-row, it has $70 \times 15 \times 4 = 4200$ points, and for the second one $50 \times 15 \times 5 = 3750$ points.

The vertical mesh lines were chosen to reduce the CPU memory requirements as well as to simplify the boundary treatment between different channels.

The computations were run on the ONERA CRAY 1 computer. The maximum file length (MFL) is about 250.000 (about 1/6 of the computer's capacity). A well-settled periodic flow field is obtained after about one rotation of the rotor (1200 s, 6000 iterations). From this evaluation, it can be seen that larger computations could be run : e.g., 2-D computations with larger blade-numbers, 3-D computations, or much more refined mesh grids if necessary.

For this compressor stage, a preliminary calculation was run with an angular speed giving an axial inlet flow in the absolute frame of reference. From the results, it was concluded that the rotor and the stator are not very well matched : the rotor outlet velocity is a bit too low, and consequently the inlet stator angle is too high. But viscous effects are not taken into account. If they were, the rotor outlet velocity would be higher in the core flow and the matching would be better. Nevertheless, such a calculation made on a domain including two cascades can give some information about the matching of these cascades which is usually achieved from a velocity triangle analysis.

In order to avoid this matching problem, the rotor angular speed was taken at a lower value, and the results can be seen on fig. 4 showing the isobaric lines (static pressure) of the flow field -at a given time t-. As they are relative to a static quantity, these lines are continuous from a cascade to the other one.

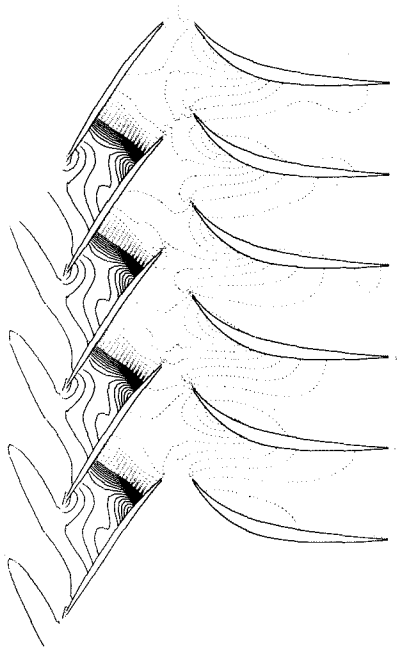


Figure 4. Constant pressure lines (compressor calculation).

The unsteady effects seem very weak : first, the influence of the stator on the rotor is almost non existent. There is a likely reason for this : this influence is of a potential type and decreases quickly in the upstream direction. On the other hand, the influence of the rotor on the stator is different : some velocity gradients in the downstream relative rotor field (due to the non uniform intensity of the shock and to the wakes) induced mainly variations of the inlet stator angle.

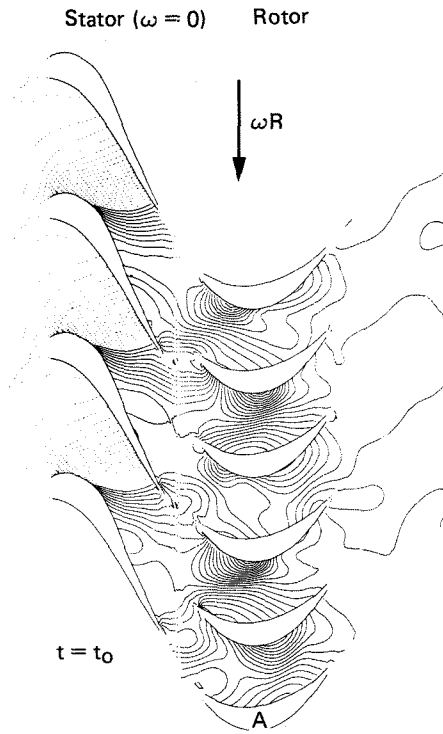


Figure 5. Constant pressure lines (turbine calculation).

For this stator (not highly loaded), the risk of separation is not very great. But in highly loaded stators, unsteady separation may be induced by these inlet angle variation. This point corresponds to the second kind of information given by such a calculation : it is possible to achieve a better approximation of the

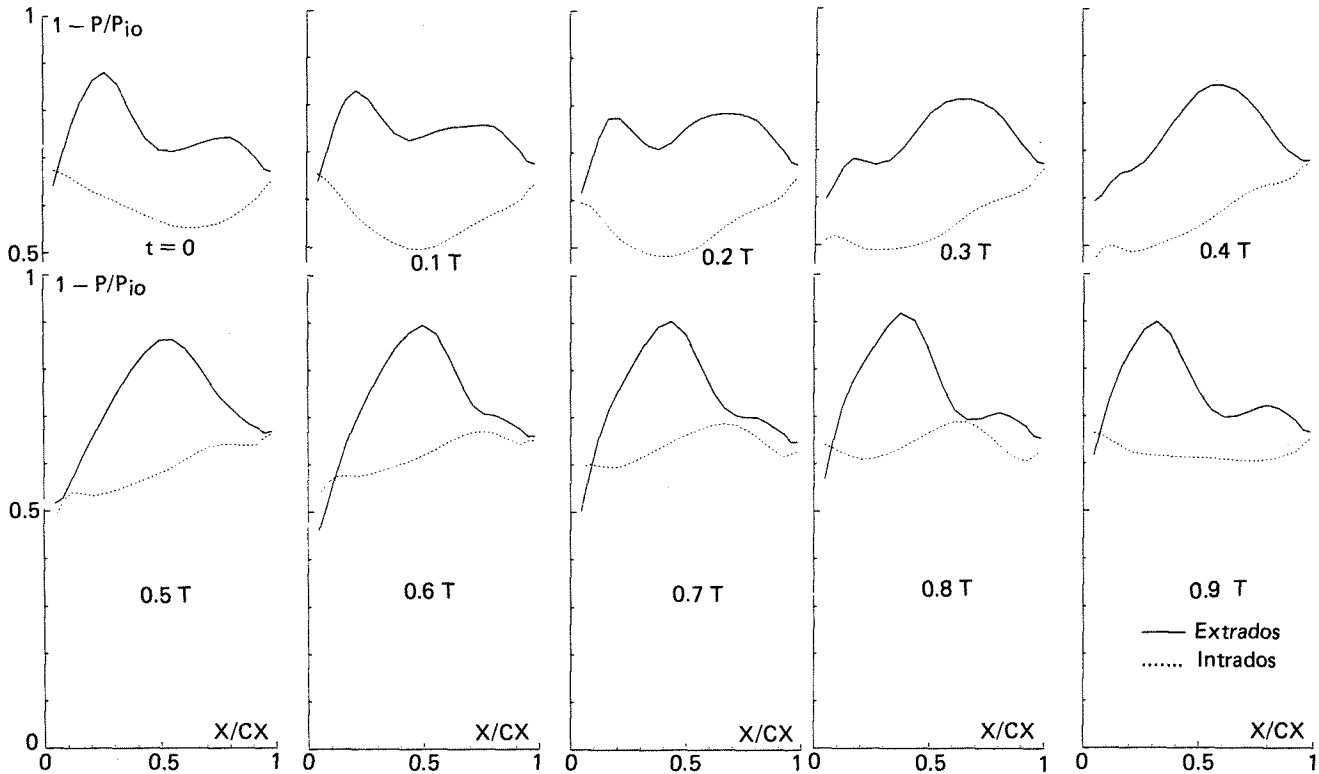


Figure 6. Static pressure distribution on rotor blade A (turbine calculation).

unsteady behaviour of turbomachinery blades, and it would be worthwhile to study how this model relates to unsteady viscous effects, aeroelasticity and acoustic problems.

IV.2. Turbine stage

A similar computation was run on a turbine stage where the main characteristics are :

- inlet axial flow Mach number : 0.22
- outlet stator flow angle : -64°
- inlet rotor flow angle : -35°
- outlet rotor flow angle : $+50^\circ$
- A.V.D.R (in the rotor only) : 0.70.

As for the compressor case, fig. 5 shows the isobaric lines of the flow field at a given time t . The potential influence of the rotor on the stator is of the same importance as the compressor one, but the influence of the stator on the rotor flow field is very drastic. The supersonic outlet stator flow gives very important unsteady effects in the rotor, as shown on fig. 6, where the static pressure distributions over a rotor blade are plotted at several moments of a period T . (T is the time required by a rotor blade to cross over a stator pitch).

IV.3 Some remarks concerning the calculation cases presented

These cases were selected in order to check the computation method. The main aims were :

- the evaluation of CPU memory and time,
- the validation of boundary conditions (slip streams, linkage of both the wheels).

Thus, the aim of the study was not to compute a very realistic case, but rather to prove that the method is able to compute unsteady flows in cascades.

Moretheless, some improvements are necessary, e.g., downstream condition to avoid non-uniformity of the flow field far from the trailing edges of the second wheel.

V. Conclusion

Theoretical approach based on the analysis of unsteady effects is an interesting step towards the improvement of numerical prediction in turbomachinery flows.

In this paper, a computation method was presented the originality of which is its ability to compute a two-dimensional unsteady flow in several rotating and non-rotating blade-rows.

Such a method could be very useful for distortion, aeroelasticity or acoustic problems, and could also be used to validate or to improve the current approximations for the mutual influence of two blade-rows.

References

1. Erdos, J.I., and Alzner, E., "Computation of Unsteady Transonic Flows Through Rotating and Stationary Cascades", NASA CR-2900, 1977.
2. Hodson, H.P., "An Inviscid Blade-to-Blade Prediction of a Wake-Generated Unsteady Flow", ASME Paper 84-GT-43.
3. Sovrano, R., "Calcul de l'écoulement Transsonique dans un Compresseur Centrifuge par une Méthode Pseudo-Instationnaire", AGARD/PEP "Centrifugal Compressors, Flow Phenomena and Performance", Bruxelles, 1980, T.P. ONERA n° 1980-42.
4. Viviani, H. et Veuillot, J.P., "Méthodes pseudo-instationnaires pour le calcul d'écoulements transsoniques", Publication ONERA n° 1978-4.
5. McCormack, R.W., and Paullay, A.J., "Computational Efficiency Achieved by Time Splitting of Finite Difference Operators", AIAA Paper 72-154, 1972.
6. Veuillot, J.P. and Meauzé, G., "A 3-D Euler Method for Internal Transonic Flows Computation with a Multi-Domain Approach", AGARD/PEP L.S. 140, ONERA T.P. n° 1985-41.
7. Joubert, H., "Supersonic Flutter in Axial Flow Compressor", Symposium IUTAM, "Unsteady Aerodynamics of Turbomachines and Propellers", Cambridge, Sept. 24-27 1984.
8. Fourmaux, A., "Unsteady Flow Calculation in Cascades", ASME Paper 86-GT-178.